nature materials

Perspective

https://doi.org/10.1038/s41563-025-02444-y

# Designing heterostructured materials

Received: 4 December 2024

Accepted: 6 November 2025

Published online: 13 January 2026

Check for updates

Hao Zhou [1], Xiaolei Wu [1,2] ✉, David Srolovitz [3] & Yuntian Zhu [1,4] ✉

Heterostructures are composed of spatially distinct zones with differing mechanical and/or physical properties. When carefully engineered, these architectures can exhibit superior performance compared with their homogeneous counterparts. However, not all heterostructures inherently lead to a pronounced improvement in properties. Realizing the full potential of complex heterostructures requires a rigorous understanding of the structure–property relationships and mechanisms related to inter-zone interactions. This knowledge is essential if the heterostructure effect is to be effectively harnessed and the overall performance of the material optimized. Here we examine the fundamental mechanisms underlying the unusual mechanical properties of heterostructured materials, highlighting the important role of interactive coupling in the heterozone boundary-affected regions. We outline strategies for evaluating the effects that arise from heterostructures, in particular the heterodeformation-induced stress. We also provide guidelines for designing heterostructured materials with optimal mechanical properties, and discuss future directions for property design and characterization development.

In recent years, heterostructured materials have attracted widespread attention in the materials community because they can be engineered to possess superior mechanical and physical properties compared with their homogeneous counterparts[1–13] (Fig. 1). For example, the heterogeneous lamella structure of titanium (Ti) has been reported to simultaneously possess the high yield strength of ultrafine-grained Ti and the high ductility of coarse-grained Ti, which overcomes the strength–ductility trade-off observed in conventional homogeneous metallic materials[14]. Gradient materials are another example that show superior mechanical properties. The biggest advantage of gradient structures is their migrating zone boundaries during tensile testing[15,16], which help to sustain the prolonged accumulation of geometrically necessary dislocations (GNDs) and statistical dislocations, thus producing extra strain hardening for a large applied strain. Harmonic structured materials have a perfect encapsulation of soft zones in a network of hard zones[11,12,17,18]. Although their reported yield strengths have been relatively low so far, they can be improved by increasing the thickness of the hard-zone network and changing the geometry of the soft zones. Other reported heterostructures include the dual-phase structure[19,20], bimodal structure[21–23], layered structure[24,25] and so on. It is noted that all of these heterostructures can be designed to improve their heterostructure effect, as discussed later.

These findings challenge our conventional understanding of materials science, including the Hall–Petch relationship[26,27] and dislocation strengthening mechanisms such as Taylor hardening[28,29], and offer an effective strategy for achieving both high strength and toughness in metallic materials. Such superior mechanical properties are enabled by a materials science principle that is absent from traditional textbooks—heterodeformation-induced (HDI) strengthening and work hardening[1].

Notably, heterostructured metals and alloys can be mass-produced at low cost using existing industrial facilities, making them highly attractive for commercial applications. For example, the heterogeneous lamella structure can be produced using cold rolling plus partial recrystallization annealing[30,31]. The heterogeneous fibrous structure can be produced using cold extrusion plus partial recrystallization annealing[32]. Other industrial processing techniques include multiple forging, heat treatment, powder metallurgy and so on. In fact, some heterostructured materials are already entering the market, for example, heterostructured lamella stainless steel[30] and heterostructured fibrous Ti[32,33], demonstrating their practical viability. These materials

[1]Department of Heterostructured Materials, Liaoning Academy of Materials, Shenyang, China. [2]State Key Laboratory of Nonlinear Mechanics, Institute of Mechanics, Chinese Academy of Sciences, Beijing, China. [3]Faculty of Engineering, The University of Hong Kong, Hong Kong, China. [4]Department of Materials Science and Engineering, City University of Hong Kong, Hong Kong, China. ✉e-mail: xlwu@imech.ac.cn; y.zhu@cityu.edu.hk

https://doi.org/10.1038/s41563-025-02444-y

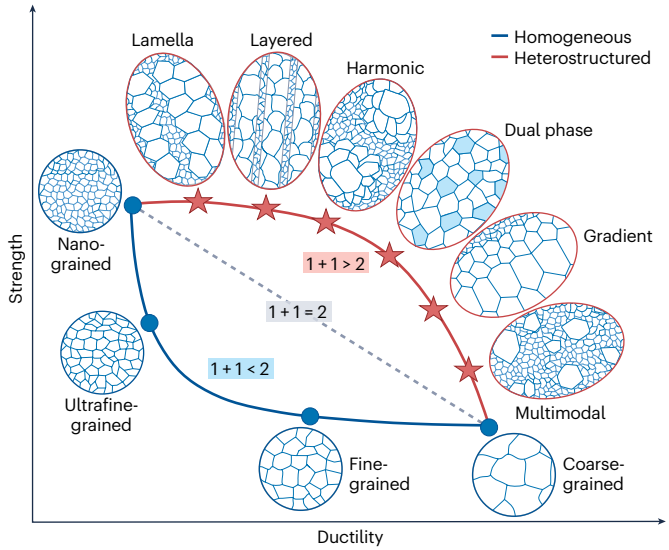


**Fig. 1 | Schematic representation of the effects of various heterostructures on the strength–ductility relationship.** For conventional homogeneous materials, ductility and strength usually show a trade-off, whereas heterostructured materials can exhibit a superior combination of both properties. $1 + 1 < 2$ indicates a lower integrated property than predicted by the rule of mixtures (ROM); $1 + 1 > 2$ denotes a higher integrated property than prediction by the ROM; the dashed straight line ($1 + 1 = 2$) means that both strength and ductility follow the ROM.

hold great promise for current and emerging high-tech industries—such as electric vehicles, drones and humanoid robots—where lightweight structures are essential.

Designing heterostructured materials should go beyond simply combining different structural components; it requires a thoughtful consideration of the beneficial effects that emerge from specific heterostructure features. Numerous heterostructured materials have been reported, but their effectiveness in enhancing mechanical properties varies widely[1]. Even within the same type of heterostructure, the performance can differ widely. Thus, intelligent design is essential and involves factors such as size, geometry and volume fraction of the heterostructured zones. In the following sections, we discuss the fundamental effects of heterostructural features that can be leveraged to improve mechanical properties, methods for evaluating these effects and practical considerations for guiding the design of heterostructured materials.

## Heterostructure effects

Although heterogeneities such as grain boundaries and second-phase particles often exist in conventional materials, they rarely generate significant heterostructure effects. This is because the heterostructure effect arises from interactive coupling between heterogeneous zones. Such interactive coupling occurs near the zone boundaries, which forms a heterozone boundary-affected region (HBAR)[1,3]. The HBAR is composed of two parts: HBAR$^{H}$, which represents the HBAR in the hard zone, and HBAR$^{S}$, which represents the HBAR in the soft zone. As discussed later, a substantial volume fraction of HBARs is essential to produce a pronounced beneficial effect.

A classic example of interactive coupling is the well-known p–n junction, where electronic interactions occur across the interface between p-type and n-type semiconductors. This electronic coupling enables a unidirectional electron flow across the junction (Fig. 2a)—a property not exhibited by either the p-type or n-type semiconductor alone. The depletion region has a width, which is a function of the charge concentrations, permittivity, equilibrium potential and external voltage. The depletion region can be considered as an HBAR. Other types of heterostructured functional material also show properties that arise from physical interactions across their heteroboundaries[13], including magnetic materials[13,34–37], thermoelectric materials[38] and ferroelectric materials[39].

For structural heterostructured materials, the interactive coupling across the heteroboundaries between the hard and soft zones is activated during deformation. Typically, the soft zones accommodate more plastic strain than the hard zones. This causes strain partitioning that inevitably leads to a strain gradient near the zone boundaries in the HBAR$^{S}$, which is accommodated by GNDs[40] (Fig. 2b). The piling up of GNDs against a zone boundary in the soft zone produces a long-range internal stress (back stress) that strengthens the soft zone. Meanwhile, at the head of a GND pile-up, a stress concentration develops which must be balanced by a forward stress at the heteroboundary.

At zone boundaries, the back stress and forward stress balance each other. The back stress strengthens the soft zone by offsetting the applied stress, while forward stress weakens the hard zone by adding to the applied stress. If these stresses fully neutralize each other across the entire volume, no strengthening will be observed in tensile tests. In reality, away from the boundaries, back stress decays slower than forward stress, preventing complete neutralization and resulting in a net strengthening effect (Fig. 2b).

The HDI stress results from the difference between the back stress and forward stress[1,3], that is, the effect of the back stress minus the effect of the forward stress. At the yield point, a high HDI stress contributes to a high yield strength. As deformation progresses, the continued building up of HDI stress produces HDI strain hardening, contributing to the retention of ductility.

HDI stresses arise at multiple structural levels, including dislocation cells, grains and heterostructured zones[2]. In conventional homogeneous metals, HDI stresses at the dislocation cell and grain levels are usually weak. By contrast, heterostructured metals show a strong HDI effect at the zone level, driven by the substantial strength differences across the zone boundaries.

The mechanical heterostructure effect originates from the piling up of GNDs in the HBAR$^{S}$ in the soft zones[24,41]. The HBAR$^{S}$ was observed from measurement of the GND density gradient near heteroboundaries using electron backscatter diffraction (EBSD)[24] (Fig. 3a), and was later confirmed via plastic strain gradient measurements using high-resolution digital image correlation (DIC)[41] (Fig. 3b). (The HBAR was initially called the interface affected zone[41].)

The heterostructure effect is produced in the HBARs, as experimentally verified[42]. Logically, the heterostructure effect should be proportional to the volume fraction of the HBARs ($f_{\mathrm{HBAR}}$):

$$\sigma_{\mathrm{HDI}} = \Delta\sigma_{\mathrm{HBAR}} f_{\mathrm{HBAR}}, \tag{1}$$

where $\sigma_{\mathrm{HDI}}$ is the HDI stress (for example, the value measured using loading–unloading–reloading methods) and $\Delta\sigma_{\mathrm{HBAR}}$ is the average stress increment caused by the HDI effect in the HBARs. Figure 3a,b shows that the HBAR encompasses both the hard- and soft-zone sides of the heteroboundary:

$$f_{\mathrm{HBAR}} = f^{\mathrm{H}}_{\mathrm{HBAR}} + f^{\mathrm{S}}_{\mathrm{HBAR}}, \tag{2}$$

where $f^{\mathrm{H}}_{\mathrm{HBAR}}$ and $f^{\mathrm{S}}_{\mathrm{HBAR}}$ are the HBAR volume fraction in the hard and soft zones, respectively. The HBAR width in the soft zone (HBAR$^{S}$) is expected to be larger than that in the hard zone according to the GND pile-up model[40] (Fig. 2b); this was verified in a Cu–Fe layered material[43].

For heterostructured materials, strengthening comes from the back stress in the soft zones, while the forward stress helps to deform, that is, softens the hard zones. Therefore, to maximize the HDI strengthening, $f^{\mathrm{S}}_{\mathrm{HBAR}}$ should be maximized. This is one of the design principles for heterostructured materials.

https://doi.org/10.1038/s41563-025-02444-y

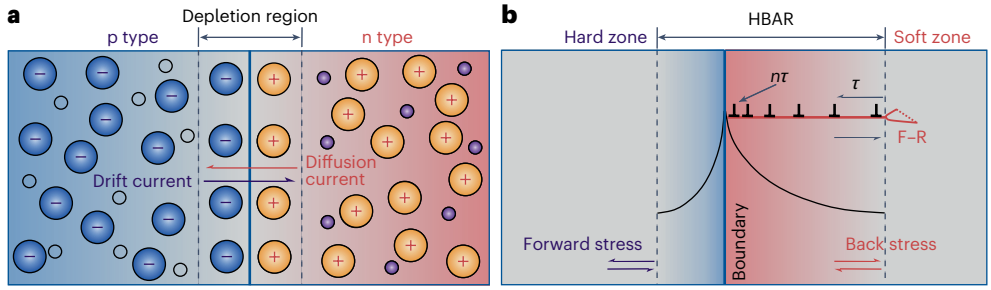


**Fig. 2 | Formation of an HBAR near a zone boundary. a**, Schematic of a depletion region, that is, an HBAR, in a p–n junction, formed by electronic coupling. **b**, Schematic of the HBAR near a hard–soft zone boundary in a structural material, formed by the piling up of GNDs (denoted by the ⊥ symbols). F–R, Frank–Read dislocation source; $\tau$, the resolved applied shear stress; $n$, the number of GNDs in the pile-up. The solid curve in the hard zone represents the profile of the forward stress; the solid curve in the soft zone represents the profile of the back stress.

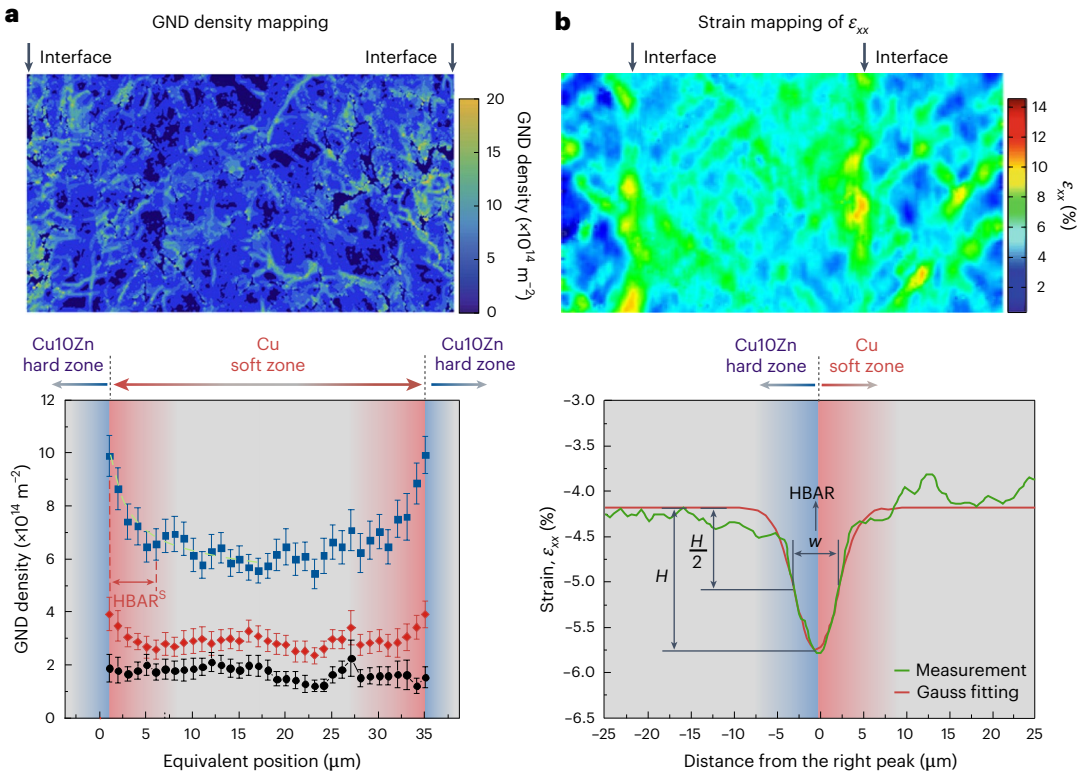


**Fig. 3 | Measurement of the HBAR. a**, EBSD observation of the density distribution of GNDs (top) and the $HBAR^S$ defined from the GND density gradient (bottom) in the soft copper layer (Cu soft zone) in a copper–bronze layered heterostructure, where the bronze comprises Cu–10 wt% Zn (Cu10Zn hard zone)[24]. Black data points are from an as-prepared tensile sample; red data points are from a sample subjected to 3% tensile strain; blue data points are from a sample subjected to 18% tensile strain; error bars mark data scatter ranges from multiple measurements for each data point; the green dashed line is a data fitting curve used for estimating the $HBAR^S$ width. **b**, Local strain distribution near the interfaces (denoted by the grey arrows) measured using DIC (top) and the HBAR defined from the strain peak at an interface in a copper–bronze layered heterostructure[41]. $\varepsilon_{xx}$, strain in the lateral direction; $H$, peak height; $w$, peak width at half-height. Panels adapted with permission from: **a**, ref. 24, Elsevier; **b**, ref. 41, Elsevier.

For most heterostructured materials, the optimum volume fraction in the soft zone is 20–30%, to achieve the best combination of strength and ductility[1,3,14]. It follows that the optimum $f^S_{HBAR}$ is equal to the volume fraction of soft zones (that is, the soft zones are fully occupied by back-stress-producing GND pile-ups), as experimentally verified in layer-structured copper–bronze laminates[41] (Fig. 4). When the thickness of the soft layer exceeds its optimum value (Fig. 4b), reducing the thickness simultaneously increases both the strength and ductility, until it reaches the optimum thickness (Fig. 4c) at which the best combination of strength and ductility is achieved. Below this optimum value (Fig. 4d), further decreasing the layer thickness reduces the ductility, although the yield strength continues to increase. The optimum thickness is when the HBARs from the opposite hetero-boundaries start to overlap in the soft zones (Fig. 4c); this occurs at ~15 μm for the copper–bronze layered structure.

The HBAR width is an important heterostructure parameter that is critical for the design of heterostructured materials. However, it remains unclear what factors affect the HBAR width[41]. It is observed that the HBAR width does not vary with the applied strain and, therefore, is probably not affected by the applied stress. It is believed that intrinsic material properties such as the stacking fault energy, shear modulus, strength difference between the soft and hard zones and the crystal structure may affect the HBAR width. A lower stacking fault energy is expected to produce a wider HBAR as it promotes GND pile-ups by

https://doi.org/10.1038/s41563-025-02444-y

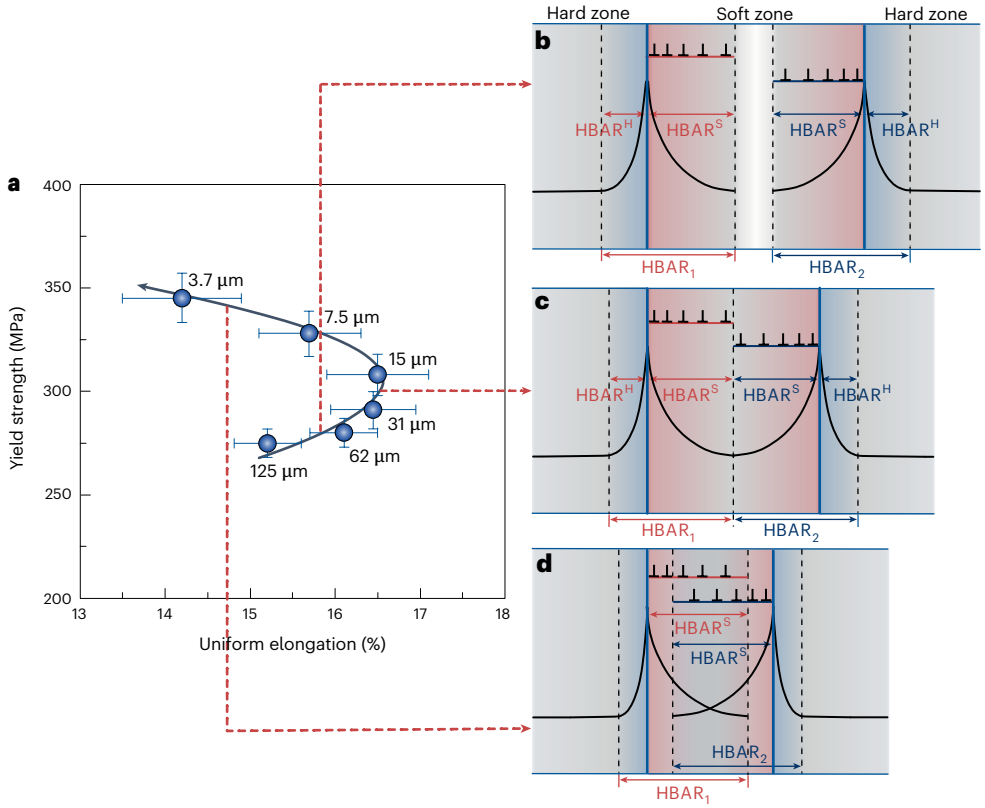


**Fig. 4 | The optimum thickness of the soft zone. a**, Variation of the strength and ductility combination as a function of the layer thickness in a copper–bronze layered structure[41]. Error bars mark data scatter ranges from multiple experiments for each data point. **b**–**d**, Schematics showing the ratio of the soft-zone thickness to the $HBAR^S$ width, where the ratio is larger than two (**b**), equal to two (**c**) and smaller than two (**d**). The optimum soft-zone thickness is two times the $HBAR^S$ width, as in **c**. $HBAR_1$ represents the first HBAR (on the left); $HBAR_2$ represents the second HBAR (on the right). Panel **a** adapted with permission from ref. 41, Elsevier.

deterring cross-slip. However, this trend may not continue once the GND pile-up activates plastic deformation in the hard zone. In addition, small precipitates and short-range ordering, if cuttable by gliding dislocations, will promote planar slip[44,45] and hence affect the HBAR width.

The optimum soft-zone volume fraction is low (20–30%) because the soft zones need to be fully constrained by hard zones to improve the yield strength, that is, soft-zone lamellae must be embedded in the hard-zone matrix. In addition, the HBAR width in the hard zone ($HBAR^H$) may plastically deform before global yielding because the forward stress effectively softens the $HBAR^H$. Therefore, it can be reasoned that the hard-zone thickness ($T_H$) must be larger than twice the width of the $HBAR^H$ to prevent percolation of plastic deformation in the hard zone (Fig. 5). In other words, the hard zones must be thick enough so that plastic deformation does not macroscopically transmit plastic strain (for example, as measured using a strain gauge). This can make the yield strength of the heterostructured material as high as that of the hard zones (as demonstrated in heterostructured lamella Ti[14]).

It is generally observed that certain heterogeneities fail to enhance the mechanical properties. A superior mechanical performance arises when the HDI stress becomes substantial. Several common reasons for the ineffectiveness of certain heterogeneities are outlined below.

First, very large soft zones (for example, soft-zone lamellae that are thicker than 20 µm) are ineffective, because the soft-zone $HBAR^S$ width is typically below 10 µm and the back stress only develops in the soft-zone $HBAR^S$. The soft-zone $HBAR^S$ width is determined by the piling up of GNDs against soft-zone boundaries.

Second, very small soft zones (for example, where the soft-zone thickness is smaller than 100 nm) are also not effective, because such small thicknesses do not provide sufficient space for GNDs to pile up. Very small soft zones produce a very high yield strength but a limited HDI strain-hardening capability and very low ductility. It should be noted that for a relatively brittle material, even a very thin soft phase may significantly enhance the toughness, but a thicker soft phase would be even better[3].

Third, the soft-zone morphology is also important for producing large heterostructure effects. As discussed above, the back stress is produced in the $HBAR^S$. As the $HBAR^S$ has a certain width, the $HBAR^S$ volume fraction is proportional to the zone boundary area per unit soft-zone volume. Therefore, the soft-zone morphology should be designed to maximize the zone boundary area per unit volume. Spherical soft zones have the lowest surface area per volume and therefore are less effective than those with high-aspect-ratio morphologies.

## Back stress, HDI stress and their measurement

The concept of back stress was initially introduced to describe the strain hardening of particle-reinforced metal matrix composites[28,46,47]. Also known as kinematic hardening, back-stress hardening is directly linked to the Bauschinger effect[48]. In the early literature[3,49–52], the back stress was similarly used to describe strain hardening. It was later realized that the back-stress concept does not fully capture the physical nature of the heterostructure effect if both the hard and soft zones deform plastically[40]. When GNDs pile up in a soft zone, they not only produce a back stress that strengthens the soft zones but also produce a forward stress that weakens the hard zones. The additional strain hardening observed in the loading–unloading–reloading (LUR) test[49] reflects a global hardening mediated by both the back stress and forward stress. Therefore, the extra stress measured using the LUR test cannot be attributed solely to the back stress[40].

https://doi.org/10.1038/s41563-025-02444-y

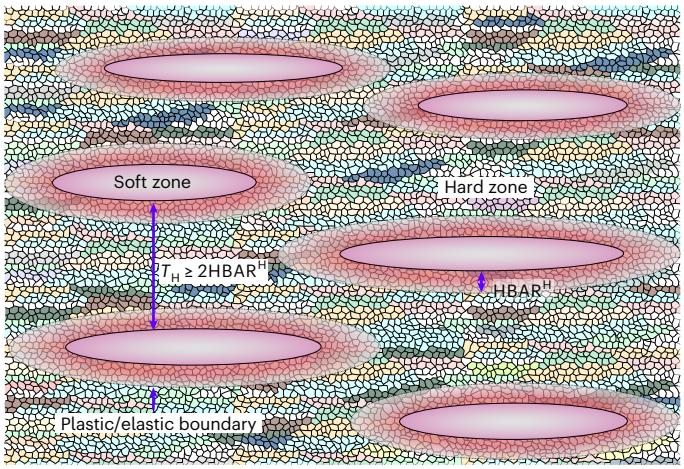


**Fig. 5** | Schematic of soft zones embedded in the hard-zone matrix and the $HBAR^H$ in the hard zone.

HDI stress was proposed to more accurately describe the extra strain hardening in heterostructured materials[40], as this hardening originates from heterogeneous deformation—that is, strain partitioning between zones. During the deformation, the soft zones sustain higher plastic strains than the hard zones, and deformation is heterogeneous. GNDs generated near zone boundaries accommodate the strain partitioning (gradient) and consequently produce back stresses in the soft zones and forward stresses in the hard zones. An LUR test measures the collective effect of back and forward stresses[49]. It should be noted that the HDI stress measured via LUR testing is not purely back stress, even though it is sometimes referred to as such. Forward stress and back stress are co-existing and inseparable; therefore, mechanical testing cannot measure them individually in heterostructured materials.

When hard zones do not undergo plastic deformation, as in the cases of ceramic-particle-reinforced metal matrix composites where the hard particles remain elastic throughout deformation, the forward stress has little influence on the mechanical behaviour of the heterostructured material. In this case, the extra stress measured in the LUR test can be largely attributed to back stress. In other words, the HDI work hardening observed in hard-particle-reinforced metal matrix composites can be considered as back-stress work hardening. For the same reason, the HDI stress at the yield point can be regarded primarily as back-stress strengthening.

The measurement of HDI stress using the LUR method has become a standard for studying the mechanical behaviour of heterostructured materials. To derive the equation for the HDI stress, it is assumed that formation of the dislocation structure is reversible during the LUR test[49]. This may not be true if the back stress is very large (which may irreversibly drive dislocations backwards during unloading). This difficulty may be resolved by doing only partial unloading—start reloading before the unloading stress reaches zero.

Since LUR strains are very small, it may be difficult to determine the linear segments on the LUR curve (this makes measurement of the HDI stress somewhat subjective). Therefore, the measured HDI stress should be considered only semiquantitative. However, a set of HDI stress data measured on different samples may be directly compared if the data are measured by the same researcher in a consistent manner. (Note that the LUR method[49] yields more consistent HDI stresses than earlier methods that use only unloading curves[50].) Readers are referred to the textbook[1,3] on how to minimize the measurement errors. A new procedure for measuring the HDI stress has recently been proposed[53], which can provide an accurate calculation of the HDI stress. However, the physical validity of this new method still needs to be probed.

## Guidelines for designing heterostructured materials

The fundamental principle for designing heterostructures with optimal mechanical properties is to promote sustained GND pile-ups at heteroboundaries over a wide strain range, thereby achieving a high yield strength and sustained HDI strain hardening. On the basis of this principle, we propose the following considerations for heterostructure design.

### Design of the zone boundary

The boundaries between soft and hard zones can be classified into two categories: sharp and diffuse (gradient) boundaries. Sharp boundaries can be easily obtained using several processing routes such as partial recrystallization of deformed metals[4], second phase formation[20] and accumulative roll bonding of immiscible metals[54]. Diffuse boundaries can be easily obtained by surface mechanical attrition[15] or by diffusion between two adjacent zones with different compositions.

GND pile-ups against a sharp boundary gradually saturate after some plastic straining, during which the HDI strain hardening will decrease[41]. This limits the HDI strain-hardening capability to improve the ductility. By contrast, diffuse boundaries migrate with applied strain (where the GNDs pile up)[15,16], leaving behind a trail of GNDs and statistically stored dislocations. This makes HDI strain hardening more effective and last longer to improve ductility. In other words, diffuse boundaries are considered better than sharp boundaries in producing HDI strain hardening and dislocation hardening. The heteroboundary must maintain cohesion and avoid failure (decohesion) during tensile deformation.

### Soft-zone morphology

The best heterostructure should maximize the heteroboundary density to provide abundant sites for GNDs to pile up. To maximize the boundary area, soft zones should adopt a lamellar or spindle geometry. However, continuous lamellae (layers) or spindles (fibres) are not ideal, as they limit the development of strain gradients along the loading direction during tensile testing, indicating the need for an optimal aspect ratio.

### Size of individual soft zones

The soft zone should be predominantly occupied by $HBAR^S$. For example, in heterogeneous lamellar structures (Fig. 4), the optimal soft-zone thickness is approximately twice the $HBAR^S$ thickness. Studies have shown that the HBAR width remains constant during tensile deformation[41] and is believed to be governed by the intrinsic properties of the material such as the shear modulus, lattice parameters and stacking fault energy. Although exact calculation of the HBAR width remains unknown, it is generally reported to be several micrometres[41,43,55]. As a rule of thumb, the thickness of soft lamellae should be in the 1–20 μm range.

### Volume fraction of soft zones

The soft-zone volume fraction should be typically below 30%, to ensure effective constraint by the hard matrix and to prevent HBARs from linking up within the matrix. A higher strength difference between soft and hard zones may allow a higher soft-zone volume fraction.

### Appropriate rates of HDI strain hardening

Is it a case of the higher the HDI strain-hardening rate the better? Contrary to intuitive expectations, increasing rate of HDI strain hardening does not always enhance the ductility. According to the Considère criterion, strain hardening only needs to merely exceed the instantaneous flow stress to suppress necking; excessively high hardening rates may, paradoxically, diminish the ductility. On the engineering stress–strain curves, the strain-hardening capacity[56] can be approximated as the difference between the ultimate tensile strength and the yield strength. As the ultimate strength typically shows limited variation for a given

metal, an elevated yield strength generally corresponds to a reduced strain-hardening capacity. An excessively high strain-hardening rate can rapidly consume this capacity, leading to early onset of necking. Therefore, it is the persistence of strain hardening, rather than its magnitude, that governs ductility. Prolonging HDI strain hardening can be achieved through microstructural strategies such as the introduction of diffuse interfaces and the activation of multiple-stage strain-hardening mechanisms[57].

### The effect of nanoscale heterogeneities

This depends on the type of heterogeneity. If the soft zones are of a nanoscale size, they are ineffective in producing back stress because there is not enough space for GNDs to pile up inside them. If the nanoscale heterogeneities are particles distributed in soft matrices, they will promote the heterostructure effect. Non-deformable nano-sized particles can block GNDs to produce back stress around them, whereas cuttable nanoparticles can promote planar slip, which also enhances GND pile-up[1,3].

## Future directions

The study of heterostructured materials faces several challenges, which also highlight key directions for future research. So far, most studies have focused on strength and ductility. Other important mechanical properties—such as fracture toughness, fatigue life, corrosion resistance, thermal stability and anisotropy—remain largely underexplored. It has been reported that gradient-structured materials show a superior fracture toughness[58]. Given the diversity of heterostructured materials and their mechanical behaviours, greater emphasis could be placed in the future on these additional properties, which are critical for engineering applications.

Second, heterostructured materials typically deform through dispersive local shear bands, a unique deformation signature that is believed to prevent large-scale strain localization and premature failure during tensile loading. However, the mechanisms that govern the nucleation and propagation of these shear bands remain unclear. In situ experiments using high-resolution DIC, EBSD and electron channelling contrast imaging (or ECCI) are essential for investigating this phenomenon.

Third, mechanical testing alone cannot distinguish back stress and forward stress during deformation. In situ synchrotron and neutron diffraction experiments are required to capture their evolution. However, extracting quantitative values of back and forward stresses from such data remains challenging, for which further theoretical analysis and software development are required.

Fourth, the width of the HBAR is a critical parameter for heterostructure design. Future research is needed to develop a predictive and reliable method for estimating the HBAR width based on the intrinsic properties of the soft and hard zones, including the stacking fault energy, shear modulus, crystal structure and lattice parameters.

In conclusion, the superior properties of heterostructured materials originate from the HBAR, in which interactive coupling between heterogeneous zones occurs. To obtain a significant heterostructural effect in heterostructured materials, it is essential to sustain appropriate HDI strain hardening over a long strain range so that ductility can be improved. An appropriate zone boundary density is desired to maximize the HBAR volume fraction while allowing enough inter-boundary distance for the GNDs to pile up. To produce a high yield strength, soft zones should be embedded in, and effectively constrained by, the hard-zone matrix.

## References


1. Zhu, Y. & Wu, X. Heterostructured materials. *Prog. Mater. Sci.* **131**, 101019 (2023).
2. Zhu, Y. et al. Heterostructured materials: superior properties from hetero-zone interaction. *Mater. Res. Lett.* **9**, 1–31 (2021).
3. Zhu, Y. & Wu, X. *Introduction to Heterostructured Materials* 1st edn (Elsevier, 2023).
4. Cheng, Z., Zhou, H., Lu, Q., Gao, H. & Lu, L. Extra strengthening and work hardening in gradient nanotwinned metals. *Science* **362**, eaau1925 (2018).
5. Li, X., Lu, L., Li, J., Zhang, X. & Gao, H. Mechanical properties and deformation mechanisms of gradient nanostructured metals and alloys. *Nat. Rev. Mater.* **5**, 706–723 (2020).
6. Fang, T. H., Li, W. L., Tao, N. R. & Lu, K. Revealing extraordinary intrinsic tensile plasticity in gradient nano-grained copper. *Science* **331**, 1587–1590 (2011).
7. Lu, K. Making strong nanomaterials ductile with gradients. *Science* **345**, 1455–1456 (2014).
8. Sathiyamoorthi, P. & Kim, H. S. High-entropy alloys with heterogeneous microstructure: processing and mechanical properties. *Prog. Mater. Sci.* **123**, 100709 (2022).
9. Wu, H. & Fan, G. An overview of tailoring strain delocalization for strength–ductility synergy. *Prog. Mater. Sci.* **113**, 100675 (2020).
10. Wei, Y. et al. Evading the strength–ductility trade-off dilemma in steel through gradient hierarchical nanotwins. *Nat. Commun.* **5**, 3580 (2014).
11. Vajpai, S. K., Ota, M., Zhang, Z. & Ameyama, K. Three-dimensionally gradient harmonic structure design: an integrated approach for high performance structural materials. *Mater. Res. Lett.* **4**, 191–197 (2016).
12. Park, H. K., Ameyama, K., Yoo, J., Hwang, H. & Kim, H. S. Additional hardening in harmonic structured materials by strain partitioning and back stress. *Mater. Res. Lett.* **6**, 261–267 (2018).
13. Zhang, X. Heterostructures: new opportunities for functional materials. *Mater. Res. Lett.* **8**, 49–59 (2020).
14. Wu, X. et al. Heterogeneous lamella structure unites ultrafine-grain strength with coarse-grain ductility. *Proc. Natl Acad. Sci. USA* **112**, 14501–14505 (2015).
15. Wu, X. L., Jiang, P., Chen, L., Yuan, F. & Zhu, Y. T. Extraordinary strain hardening by gradient structure. *Proc. Natl Acad. Sci. USA* **111**, 7197–7201 (2014).
16. Yang, M.-X. et al. Residual stress provides significant strengthening and ductility in gradient structured materials. *Mater. Res. Lett.* **7**, 433–438 (2019).
17. Sawangrat, C., Kato, S., Orlov, D. & Ameyama, K. Harmonic-structured copper: performance and proof of fabrication concept based on severe plastic deformation of powders. *J. Mater. Sci.* **49**, 6579–6585 (2014).
18. Nagata, M., Horikawa, N., Kawabata, M. & Ameyama, K. Effects of microstructure on mechanical properties of harmonic structure designed pure Ni. *Mater. Trans.* **60**, 1914–1920 (2019).
19. Calcagnotto, M., Adachi, Y., Ponge, D. & Raabe, D. Deformation and fracture mechanisms in fine- and ultrafine-grained ferrite/martensite dual-phase steels and the effect of aging. *Acta Mater.* **59**, 658–670 (2011).
20. Li, Z., Pradeep, K. G., Deng, Y., Raabe, D. & Tasan, C. C. Metastable high-entropy dual-phase alloys overcome the strength–ductility trade-off. *Nature* **534**, 227–230 (2016).
21. Wang, Y., Chen, M., Zhou, F. & Ma, E. High tensile ductility in a nanostructured metal. *Nature* **419**, 912–915 (2002).
22. Han, B. Q., Lavernia, E. J., Lee, Z., Nutt, S. & Witkin, D. Deformation behavior of bimodal nanostructured 5083 Al alloys. *Metall. Mater. Trans. A* **36**, 957–965 (2005).
23. Han, B. Q., Huang, J. Y., Zhu, Y. T. & Lavernia, E. J. Strain rate dependence of properties of cryomilled bimodal 5083 Al alloys. *Acta Mater.* **54**, 3015–3024 (2006).
24. Ma, X. et al. Mechanical properties in copper/bronze laminates: role of interfaces. *Acta Mater.* **116**, 43–52 (2016).
25. Ma, X. L. et al. Strain hardening and ductility in a coarse-grain/nanostructure laminate material. *Scr. Mater.* **103**, 57–60 (2015).

26. Hall, E. O. The deformation and ageing of mild steel: III discussion of results. *Proc. Phys. Soc. B* **64**, 747 (1951).
27. Petch, N. J. The cleavage strength of polycrystals. *J. Iron Steel Inst.* **174**, 25–28 (1953).
28. Ashby, M. F. The deformation of plastically non-homogeneous materials. *Philos. Mag.* **21**, 399–424 (1970).
29. Gao, H., Huang, Y., Nix, W. D. & Hutchinson, J. W. Mechanism-based strain gradient plasticity – I. Theory. *J. Mech. Phys. Solids* **47**, 1239–1263 (1999).
30. Li, J., Cao, Y., Gao, B., Li, Y. & Zhu, Y. Superior strength and ductility of 316L stainless steel with heterogeneous lamella structure. *J. Mater. Sci.* **53**, 10442–10456 (2018).
31. Cheng, Q. et al. Optimizing strength–ductility synergy in lightweight steel via heterogeneous design: discontinuous fibrous ferrite. *Mater. Res. Lett.* **12**, 947–955 (2024).
32. Wang, R. et al. High strength titanium with fibrous grain for advanced bone regeneration. *Adv. Sci.* **10**, 2207698 (2023).
33. Wang, R. et al. Crystallographic plane-induced selective mineralization of nanohydroxyapatite on fibrous-grained titanium promotes osteointegration and biocorrosion resistance. *Biomaterials* **313**, 122800 (2025).
34. Lou, L. et al. Directional magnetization reversal enables ultrahigh energy density in gradient nanostructures. *Adv. Mater.* **33**, 2102800 (2021).
35. Li, X. et al. Novel bimorphological anisotropic bulk nanocomposite materials with high energy products. *Adv. Mater.* **29**, 1606430 (2017).
36. Li, X. et al. Controllably manipulating three-dimensional hybrid nanostructures for bulk nanocomposites with large energy products. *Nano Lett.* **17**, 2985–2993 (2017).
37. Li, H. et al. Three-dimensional self-assembly of core/shell-like nanostructures for high-performance nanocomposite permanent magnets. *Nano Lett.* **16**, 5631–5638 (2016).
38. Biswas, K. et al. High-performance bulk thermoelectrics with all-scale hierarchical architectures. *Nature* **489**, 414–418 (2012); erratum **490**, 570 (2012).
39. Li, F. et al. Ultrahigh piezoelectricity in ferroelectric ceramics by design. *Nat. Mater.* **17**, 349–354 (2018).
40. Zhu, Y. & Wu, X. Perspective on hetero-deformation induced (HDI) hardening and back stress. *Mater. Res. Lett.* **7**, 393–398 (2019).
41. Huang, C. X. et al. Interface affected zone for optimal strength and ductility in heterogeneous laminate. *Mater. Today* **21**, 713–719 (2018).
42. Wang, Y. F. et al. Hetero-deformation induced (HDI) hardening does not increase linearly with strain gradient. *Scr. Mater.* **174**, 19–23 (2020).
43. Ran, H. et al. Superior strength–ductility combination resulted from hetero-zone boundary affected region in Cu–Fe layered material. *J. Mater. Sci. Technol.* **181**, 209–219 (2024).
44. Gerold, V. & Karnthaler, H. P. On the origin of planar slip in f.c.c alloys. *Acta Metall.* **37**, 2177–2183 (1989).
45. Steffens, T., Schwink, C., Korner, A. & Karnthaler, H. P. Transmission electron microscopy study of the stacking-fault energy and dislocation-structure in CuMn alloys. *Philos. Mag. A* **56**, 161–173 (1987).
46. Ashby, M. F. Work hardening of dispersion-hardened crystals. *Philos. Mag.* **14**, 1157–1178 (1966).
47. Tanaka, K. & Mori, T. Hardening of crystals by non-deforming particles and fibres. *Acta Metall.* **18**, 931–941 (1970).
48. Bouaziz, O., Barbier, D., Embury, J. D. & Badinier, G. An extension of the Kocks–Mecking model of work hardening to include kinematic hardening and its application to solutes in ferrite. *Philos. Mag.* **93**, 247–255 (2013).
49. Yang, M., Pan, Y., Yuan, F., Zhu, Y. & Wu, X. Back stress strengthening and strain hardening in gradient structure. *Mater. Res. Lett.* **4**, 145–151 (2016).
50. Feaugas, X. On the origin of the tensile flow stress in the stainless steel AISI 316L at 300 K: back stress and effective stress. *Acta Mater.* **47**, 3617–3632 (1999).
51. Helbert, A. L., Feaugas, X. & Clavel, M. Effects of microstructural parameters and back stress on damage mechanisms in α/β titanium alloys. *Acta Mater.* **46**, 939–951 (1998).
52. Hong, S. I. & Laird, C. Cyclic deformation-behavior of Cu–16 at.% Al single-crystals. Part III: friction stress and back stress behavior. *Mater. Sci. Eng. A* **128**, 155–169 (1990).
53. Chen, R. et al. Hetero-deformation induced (HDI) stress measurement from the plastic dissipation in the hysteresis loops. *Mater. Res. Lett.* **13**, 248–255 (2025).
54. Ardeljan, M., Savage, D. J., Kumar, A., Beyerlein, I. J. & Knezevic, M. The plasticity of highly oriented nano-layered Zr/Nb composites. *Acta Mater.* **115**, 189–203 (2016).
55. Wang, Y., Zhu, Y., Yu, Z., Zhao, J. & Wei, Y. Hetero-zone boundary affected region: a primary microstructural factor controlling extra work hardening in heterostructure. *Acta Mater.* **241**, 118395 (2022).
56. Dong, X. X., Shen, Y. F. & Zhu, Y. T. Moderating strain hardening rate to produce high ductility and high strength in a medium carbon TRIP steel. *Mater. Res. Lett.* **11**, 69–75 (2023).
57. Shi, P. et al. Multistage work hardening assisted by multi-type twinning in ultrafine-grained heterostructural eutectic high-entropy alloys. *Mater. Today* **41**, 62–71 (2020).
58. Cao, R. et al. On the exceptional damage-tolerance of gradient metallic materials. *Mater. Today* **32**, 94–107 (2020).


## Acknowledgements

This work was supported by the National Key R&D Program of China (2021YFA1200202), the National Natural Science Foundation of China (52571139), the Guangdong Basic and Applied Basic Research Foundation (2024B1515130001) and the Hong Kong Research Grants Council (GRF 11214121).

## Competing interests

The authors declare no competing interests.

## Additional information

**Correspondence** should be addressed to Xiaolei Wu or Yuntian Zhu.

**Peer review information** *Nature Materials* thanks Zhaoping Lu and the other, anonymous, reviewer(s) for their contribution to the peer review of this work.